Drug Design, Development and Therapy

Dovepress
Taylor & Francis Group

Open Access Full Text Article

ORIGINAL RESEARCH

Huanglian Ejiao Decoction Alleviates Ulcerative Colitis in Mice Through Regulating the Gut Microbiota and Inhibiting the Ratio of Th1 and Th2 Cells

Jingyi Tang[1,2,*], Yingnan Hu[1,3,*], Jintao Fang[1,*], Weihan Zhu[1,*], Wenjun Xu[1], Dian Yu[1], Zhipeng Zheng[4], Qiujing Zhou[4], Huiying Fu[4], Wei Zhang[1,4]

[1]The Second Clinical Medical College of Zhejiang Chinese Medical University, Hangzhou, 310053, People's Republic of China; [2]Lanxi Hospital of Traditional Chinese Medicine, Jinhua, 321100, People's Republic of China; [3]The Sixth Affiliated Hospital, Sun Yat-Sen University, Guangzhou, 510510, People's Republic of China; [4]The Second Affiliated Hospital of Zhejiang Chinese Medical University, Hangzhou, 310005, People's Republic of China

*These authors contributed equally to this work

Correspondence: Wei Zhang; Huiying Fu, Email zhangweils1968@163.com; fhy131@126.com

Background: Huanglian-ejiao decoction (HED) is a Chinese traditional medicinal formula evolved from the Shanghan Lun (Treatise on Febrile Diseases). However, HED ultimate mechanism of action remained indistinct. Therefore, this study aimed to investigate whether HED could exert anti-inflammatory effects on 2,4,6-Trinitrobenzenesulfonic acid (TNBS)-induced colitis (UC) model through the regulation of $CD4^+$T subsets and gut microbiota.

Methods: Fifty-eight major compounds in HED were identified by UPLC-Q-TOF/MS. The therapeutic efficacy of HED on UC was assessed by evaluating survival rate and so on. Flow cytometry was employed to assay the percentages of $CD4^+$T cell. RT-PCR and Western blot took advantage of detecting transcription factors, inflammatory factors, and tight junction proteins. Transcriptome sequencing was performed on colon tissue and 16S rRNA gene sequencing was enforced on intestinal contents.

Results: The administration of HED enhanced the survival rate of colitis mice, significantly restored body weight, DAI score, colon weight and index, spleen weight and index. HED effectively reshaped intestinal barrier dysfunction, inhibited the ratio of Th1 to Th2 cells, and preserved Th2/Th1 and Tregs/Th17 balance. Moreover, HED notably decreased the secretion of transcription factors and related cytokines. Interestingly, HED also exerts regulatory effects on gut dysbiosis by cumulative the plenteous of beneficial probiotics like Lactobacillus and Bacteroides, while inhibiting the overgrowth of opportunistic pathogens such as Helicobacter.

Conclusion: The regulation of Th2/Th1 and Tregs/Th17 cell balance, as well as the modulation of gut microbiota by HED, provides further experimental evidence for the feasibility of its treatment of UC.

Keywords: HED, ulcerative colitis, Th2/Th1, Treg/Th17, gut microbiota

Introduction

Ulcerative colitis (UC) is a nonspecific, chronic inflammatory bowel disease (IBD) involving the submucosa and mucosa of the colon and rectum, which is primarily characterized by diarrhea (with bowel movement frequency ranging from 2–10 times per day) accompanied by the presence of blood, pus and mucus in the feces.[1] This disease can occur at any age but is more ubiquitous in middle-aged and young people aged 20–40 years.[2] The current therapeutic efficacy of UC is considerably limited due to its multifactorial etiology and pathogenic mechanism, encompassing genetic predisposition, immune dysregulation, gut microbiota imbalances, smoking habits, psychological stressors, and dietary patterns.[3] The conventional treatment of UC includes anti-inflammatory drugs such as immunosuppressant therapies, mesalazine derivatives and corticosteroids.[4] However, the efficacy of these treatments is limited in achieving the therapeutic goals

Received: 31 July 2024
Accepted: 6 January 2025
Published: 17 January 2025

for UC, which include reducing inflammatory symptoms, inducing or maintaining clinical and endoscopic remission, and minimizing disability.[5] Consequently, some patients may require colon surgery due to insufficient effectiveness or severe complications.

The pathogenesis of UC remains a contentious topic, characterized by its intricate nature. $CD4^+$T cells play a pivotal factor in regulating overall wellness and sickness, while restoring the equilibrium of $CD4^+$T cells aids in maintaining intestinal mucosal homeostasis.[6] The immunology community has discovered that activation is necessary for the discrimination of naive $CD4^+$T cells into Th1, Th2, Th17, and Tregs, thereby coordinating various adaptive immune responses. Furthermore, the gut microbiota provides numerous beneficial functions for the host encompassing immunity, metabolism, diseases etc., with its most dramatic function being its influence on the host's immune system. On the one hand, it promotes early development and maturation of the immune system; on the other hand, it helps maintain the completeness of the intestinal barrier as well as regulate and sustain immune balance within the host.[7] The gut microbiota and its microbial metabolites can induce differentiation of $CD4^+$T cells through direct or indirect mechanisms to maintain immune homeostasis. Research data demonstrate that colitis induced by TNBS triggers Th1 and Th17 immune responses, resulting in the expression of numerous pro-inflammatory cytokines.[8] These immune responses of Th1 and Th17 lead to infiltration of inflammatory cells such as neutrophils, causing severe symptoms such as weight-loss, diarrhea and rectal prolapse. Both induced and spontaneous experimental models of colitis have authorized the involvement of inflammatory processes mediated by Th1 and Th2.[9] Recent evidence suggests that cytokines (secreted by Th2 and Tregs) have the ability to suppress the secretion of cytokines related to Th1/Th17 pathways, thereby alleviating IBD symptoms. Restoring the balance between Th1/Th2 and Th17/Tregs may represent an efficacious therapeutic approach for UC.[10]

HED is a traditional Chinese medicinal (TCM) prescription, initially documented in Zhang Zhongjing's Treatise on Cold Disease during the Han Dynasty. UC falls under TCM category "diarrhea, intestinal wind" with specific syndrome types including liver-kidney deficiency syndrome, dampness-toxin nostalgia syndrome, Yin-blood deficiency syndrome eg.[11,12] The composition of HED includes Coptidis Rhizoma, Scutellariae Radix, Paeonia lactiflora Pall and Donkey-hide Gelatin. HED was changed by Gegen Qinlian decoction (GQD), which removed Gegen and licorice, and added Paeonia lactiflora pall and Donkey-hide Gelatin. HED has the potential to ameliorate colonic inflammation through restructuring of gut flora, specifically by regulating the $CD4^+$T cell subsets balance associated with gut microbiota.[13] White peony root has the effect of treating pus and blood and anti-inflammatory properties, and Colla corii asini has the effect of stopping bleeding and anti-inflammatory effect.[14] HED has a variety of effective chemical components, such as berberine, paeoniflorin, and baicalin.[15] Berberine has been utilized to cure intestinal infection and inflammation.[16] Paeoniflorin possesses extensive anti-inflammatory and immune regulatory effects.[17] Baicalin enhances the completeness of the intestinal barrier, exhibits antioxidant and anti-inflammatory properties, and promotes a healthy gut microbiota in individuals with UC.[18] In TCM, HED demonstrates efficacy in treating hematochezia, abdominal pain, and diarrhea, aligning with the Yin deficiency and blood deficiency characteristic of UC. HED's therapeutic approach for ulcerative colitis (UC) aligns with traditional Chinese medicine (TCM) dialectics, particularly by addressing Yin-blood deficiencies. This alignment is supported by both theoretical underpinnings and clinically proven effectiveness. In addition, HED efficacy has been explored in our previous experiment. However, the underlying mechanism of action remained obscure. Furthermore, the potential role of HED in restoring $CD4^+$T cell balance during intestinal inflammation and its implications for the treatment of UC have not yet been reported. Thus, this study aimed to further investigate the therapeutic effects and mechanisms of HED on TNBS-induced UC mice by investigating its impact on gut microbiota and $CD4^+$T cells.

Materials and Methods

Composition and Preparation of HED

HED was procured from the Traditional Chinese Medicine (TCM) Out-patient Department at Zhejiang Chinese Medicine University (Zhejiang, China), according to the original prescription dosage of Shanghanlun, made with the following four herbs: Coptidis Rhizoma (Huanglian, 12 g), Scutellariae Radix (Huangqin, 6 g), Paeonia Lactiflora Pall (Baishao, 6 g), and Donkey-hide Gelatin (Ejiao, 9 g), in a ratio of 4:2:2:3[19] which corresponds to the daily clinical dosage for humans, based on the equivalent dose ratio table, the dosage administered to mice is 9.1 times that of general humans (60kg). As a

result, the low and high doses of HED for mice are approximately 2.5025 g crude herbs/kg and 10.01 g crude herbs/kg, respectively (analogous to half and twice the common dose for clinical patients). TCM was drenched in double distilled water (ddH_2O) for 90 min, boiled over a fire for 40 minutes, simmered on low heat for 90 min, and then filtered. This process was iterative three times to extract the desired volume of solution. The extracted solution was subsequently evaporated and condensed into a final low dose of 98.9 mL and a high dose of 24.7 mL. Finally, the solution was sealed and deposited in a refrigerator at a temperature of 4°C.

Component Analysis of HED

The UPLC-Q-TOF/MS (Waters SYNAPT G2-Si, Milford, MA, USA) with Unifi/Qi software (Waters, Milford, MA, USA) was accomplished for the qualitative analysis and data processing. The liquid phases comprised water (A) containing 0.1% formic acid and acetonitrile (B) 0.1% formic acid, and the elution time was set at 35 minutes, whose conditions were as follows: A: 0–2 min; 5–100% A: 2–32 min; 100% A: 32–33 min; 5% A: 33–35 min. The pillar temperature was held steady at 35 °C throughout and the flux rate was 0.3 mL/min with the injection volume of 2ul. The specimens were primarily deliquescent in 75% ethanol, and the epipelagic sample was selected as the test solution following filtration through a membrane (0.22 μm). The mass spectra were procured by electrospray ionization (ESI) source by scanning negative and positive ions mode in the scope of m/z 50 ~ 1200 Da. The calibration of the mass spectrometer calibration was conducted utilizing sodium formate, and real-time mass correction was performed using leucine enkephalin (negative mode: 554.2615 m/z; positive mode 556.2771 m/z). The following parameter settings were performed: capillary voltage, 2.5 kV (negative) and 3 kV (positive); desolvation and ion source temperature, 500 °C and 120 °C; cone voltage and collision energy, 40 V and 15–45 V; scan time, 0.2 s; scan range, 50–1200 Da; desolvation and cone gas flow rate, 1000 L/h and 100 L/h.

Animals

A total of Specific Pathogen Free (SPF) 50 male Balb/c mice male Balb/c mice (6–8 weeks old; weighing 22±2 g) were acquired from Beijing HFK Bio-Technology. CO., Ltd (Animal License No. SCXK, Beijing, 20230811Abzz0100999606). The mice resided in a controlled SPF laboratory environment with a 12 hour-dark/12 hour-light cycle and temperature maintained at 21±1°C, which was provided with standard mouse diet and unrestricted access to tap water for an acclimation period of one week. The procedures were executed compliance with the Guidelines for Care and Use of Laboratory Animals of Zhejiang Chinese Medical University (IACUC-20220307-22).

Experimental Model of UC

The experimental mice were mildly anesthetized with 0.3% pentobarbital sodium by intraperitoneal injection (50 mg/kg).[20] Then, the mice were placed in prone position and the cannula surface of the intravenous indentor needle was smeared with paraffin oil and gently inserted into the colon through the anus. When the tip of the cannula was inserted about 4 cm from the anus, the inner core of the trocar with a syringe was immediately inserted into the cannula. At the same time, mice were inverted and slowly injected with TNBS (No. 20101002, Sigma-Aldrich) solution at the dose of 100 mg per kg of body weight.[21] Then the trocar was pulled out, and the mouse tail was held in an inverted position for 60 seconds to ensure better absorption and distribution of the injected solution in the intestine. Finally, the mouse head tilted down to the natural recovery, with normal saline scrub off the anus outflow of enteric liquid, to prevent the mice from licking poisoning. Then, the mice were put back into the cage to eat and drink freely.

Animal Administration and Sampling

The 50 mice were erratically allocated into five groups: the Control (CON), TNBS, HED-L, HED-H, sulfasalazine (Salazosulfapyridine; SASP) groups. The CON group was not treated, and the other four groups were intrarectally injected with TNBS to induce UC. The mice in the CON and TNBS groups were orally administered ddH_2O, while the HED-L and HED-H groups orally received 2.50 and 10.01 mg/kg of HED, and the SASP group was orally treated with 500 mg/kg of SASP (No. H31020557, Tianping Pharmaceutical, Shanghai, China).[22] The drugs were administered on the first day after modeling and continued for 6 days, 0.4mL/20g, once a day. On the 6th day after modeling, the mice were euthanized with carbon dioxide and blood was taken from the heart. The colon of mice was extracted by laparotomy

along the midabdominal line. Mice colons were taken for flow cytometry, part of the colon was taken for pathological HE, and the rest was frozen and stored for real-time polymerase chain reaction (qPCR) detection and Western blot detection. Colonic feces were frozen at −80 °C for 16S rRNA gene sequencing.

Disease Activity Index

From the modeling date, the mental state, eating, drinking, activity and body hair of the mice were observed and recorded every day.[23,24] The shape of stool and the condition of stool blood were observed. Weight loss was the disparity between initial weight and measured weight, while diarrhea was characterized by the absence of fecal pellet formation and continuous presence of liquid fecal material in the colon. DAI scoring = (weight loss score)/3 + (Fecal trait score)/3+ (blood stool score)/3. (Table 1) In the DAI score, stool bleeding was divided into normal (0 points), occult blood positive (1–3 points) and overt bleeding (4 points), and occult blood positive was further subdivided into +, ++ and +++, which were detected by o-toluidine method. + indicated mild occult blood, which changed from light green to blue after adding reagent for 10 seconds. ++ indicates moderate occult blood that changes in color to blue and gradually changes to blue-brown, and +++ indicates severe occult blood that changes in color to blue-brown and gradually changes to blue-black.

Transcriptome Sequencing Analysis

The RNA of colonic tissue was isolated from colonic tissues of mice in CON, TNBS, and HED-H groups and its integrity confirmed by formol agarose gel electrophoresis (Contains formaldehyde) and Bioanalyzer 2100 (Agilent, CA, USA). The NanoDrop ND-1000 (NanoDrop, Wilmington, DE, USA) was used to detect the amount and purity of total RNA. Total RNA > 1 μg, RNA integrity number (RIN) > 7.0, Concentration > 50 ng/μL meet the criteria for RNA library inclusion. Following cluster generation, the RNA libraries were sequenced on the illumina NovaseqTM 6000 platform by LC Bio Technology CO, Ltd (Hangzhou, China). After the transcriptome sequencing, we manipulated the OmicStudio tools (https://www.omicstudio.cn/tool) to analyze the raw data constitute the Kyoto Encyclopaedia of Genes and Genomes (KEGG) and Gene Ontology (GO) enrichment analyses.

Isolation of Intestinal Immune Cells

The isolation technique of lamina propria lymph nodes were experimentally optimized and refined, but with some specific modifications.[25] The colon was opened longitudinally, kept in 3 mL HBSS (Thermo Fisher Scientific) with 5 mM EDTA (Thermo Fisher Scientific) and 2% FBS (Omega Scientific) and oscillated at 37 °C for 30 min. Then, the tissue was washed twice with prechilled PBS (Biosharp), kept in 1.2 mL RPMI 1640 (Thermo Fisher Scientific) and sheared into tiny pieces. Next, 1 mL RPMI 1640 embracing 10% FBS, and 0.4 U/mL Dispase II (Solarbio), 1 mg/mL collagenase III (Solarbio) and 20 μg/mL DNase I (Beyotime) were added. The digestion was carried out at 37 °C for 45 min by shaking, and then the sample was filtered through 70 μm nylon mesh to obtain a tissue suspension.[26–28]

Table 1 The DAI Scoring Standards

Weight Loss (%)	Stool Consistency	Presence of Gross Bleeding or Bloodstain	Score
<0	Normal	Negative	0
1–5	/	+	1
5–10	Loose	++	2
10–20	/	+++	3
>20	Diarrhea	Rectal Hemorrhoea	4

Flow Cytometry

The antibodies used in the flow cytometry (Anti-CD45-PE-cy7, anti-CD4-FITC, anti-T-bet-BV421, anti-GATA-3-BB700, anti-RORγT-AF647, anti-Foxp3-PE, anti-CD25-BV605 and Transcription Factor Buffer Set (TF)) were purchased from BD Biosciences (San Jose, CA, USA). The isolated mononuclear cell suspension was prepared, washed, mixed with antibodies CD45-PE-Cy7, CD4-FITC and CD25-BV605, incubated in dark light for 15 min, washed with PBS, then incubated with film TF at −4 °C for 60 min, and washed with PBS. The mixture of T-bet-BV421/GATA-3-BB700 was added, incubated at −4 °C degrees away from light for 60 min, washed, fixed, and analyzed by flow cytometry (BD Biosciences).[29]

Western Blot Analysis

The antibodies used in WB (anti-IL-1β (GB11113, Servicebio, Wuhan, China), anti-GAPDH (GB11002, Servicebio, Wuhan, China), anti-ZO-1 (bs-1329R, Bioss, Woburn, MA, USA), anti-Occludin (#91131, CST, Danvers, MA, USA), anti-IL-6 (DF6087, Affinity Biosciences, Jiangsu, China). Anti-IL-4 (P05112), anti-IL-10 (P22301), anti-IL-17A (Q16552) and anti-β-actin (P60709) were purchased from Proteintech Company in Wuhan, China. Briefly, proteins of colon were lysed and extracted using RIPA buffer, and protein quantification was measured using the BSA method. After blocking with 5% defatted milk, membranes were incubated with primary antibodies containing anti-ZO-1 (1:1000), anti-Occludin (1:500), and anti-IL-1β (1:500) for 1 h overnight at 4 °C. Then, the second antibody was added dropwise at room temperature incubating 2 h, and after that, washed Tris-buffered saline (TBST) 3 times. Finally, the FluorChem R (ProteinSimple, USA) and ImageJ analysis software 1.4.3.67 (National Institutes of Health, Bethesda, MD, USA) were wielded for band visualization and quantification.

RNA Extraction and Real-Time PCR

Total RNA was extracted out from snap frozen (at −80 °C) intestine tissue using a TRIzol-based method. Reverse transcription was performed using a HiScript III RT SuperMix for qPCR kit abiding by the manufacturer's instructions. Primers were designed for qRT-PCR based on the 16S rRNA gene sequences available in the National Center for Biotechnology Information (NCBI) databases, and (Table 2). The amplification primers and reagent on top were furnished by Accurate Biotechnology (China) CO., LTD (Shanghai, China). The experimental results were calculated using the $2^{-\Delta\Delta Ct}$ formula.

Table 2 Primer Sequences of the Genes Used for qRT-PCR

Gene	Forward Primer	Reverse Primer	Gene ID
β-actin	CATCCGTAAAGACCTCTATGCCAAC	ATGGAGCCACCGATCCACA	14433
ZO-1	ACCAGATGTGGATTTACCCGTCA	ACATCATTTCCACCAGCTAGTCG	21872
Occludin	GGCAAGCGATCATACCCAGA	GGCAAGCGATCATACCCAGA	18260
IL-4	ACGGAGATGGATGTGCCAAAC	AGCACCTTGGAAGCCCTACAGA	16189
IL-6	TGATGGATGCTACCAAACTGGA	TCTCTCTGAAGGACTCTGGCT	16193
IL-10	TCTCTCTGAAGGACTCTGGCT	TCACTCTTCACCTGCTCCAC	16153
IL-17A	TCAGACTACCTCAACCGTTCCA	CTTTCCCTCCGCATTGACACA	16171
IL-1β	TGGTGTGTGACGTTCCCATT	TGTCGTTGCTTGGTTCTCCT	16176
T-bet	CCACCTGTTGTGGTCCAAGT	TGTAATGGCTTGTGGGCTCC	57765
Gata-3	CTCGGCCATTCGTACATGGAA	CATACCTGGCTCCCGTGGTG	14462

https://doi.org/10.2147/DDDT.S468608

Investigation of Gut Microbiota by 16S rRNA Gene Sequencing

Fecal samples were acquired from the colon contents to extract genomic DNA of the gut microbiota and accomplished 16S rRNA Gene Sequencing (LC Bio Technology CO., Ltd, Hangzhou, China). The sequencing analysis process put to avail QIIME 2 version, which was tantamount to clustering with 100% similarity, and next invoked the split amplification de-noising algorithm (DADA2) to de-noise the data, excluded the redundancy, and acquired the features. Pursuant analysis results were reliant on features data. We utilized the OmicStudio tool to constitute Correlation Network diagram, Violin plot and Clustering correlation heatmap at OmicStudio.

Statistical Analysis

The data were denoted as mean ± standard error of mean (SEM). The *t*-test was exploited for pairwise comparisons, and one-way ANOVA of variance followed by Tukey's tests when groups were more than two. $P \leq 0.05$ is an enormous difference.

Result

Chemical Compounds of HED Was Identified

The base peak intensity (BPI) chromatogram profile of HED included positive and negative ions (Figure 1). A total of 58 compounds (1–58) were identified by the Unifi/Qi software, binding the fragment ions and the empirical molecular formulas (Table 3). Forty-one major components were detected in the positive ions and 33 major components were detected in the negative ions, of which 16 major components were detected by both positive and negative ions. In addition, the mass spectrometry analysis of the formula was obtained by the analysis of Coptidis rhizoma, Scutellaria baicalensis and Paeonia lactiflora pall. Ejiao, a traditional Chinese medicinal material sourced from donkey skin, primarily consists of high-molecular-weight collagen. However, the complex structure and thermal instability of this collagen present substantial obstacles for mass spectrometry analysis, making Ejiao unsuitable for this type of analytical technique. Berberine, Tetrandrine, Coptisine and Groenlandicine found in Coptidis rhizoma; Baicalin, Baicalein and Chrysin present in Scutellaria baicalensis; as well as Paeoniflorin, Albiflorin, and Lactiflorin derived from Paeonia lactiflora pall were well-established active ingredients. The functions of several of these components were intricately linked to T-cell differentiation and the composition of gut microbiota, for instance, Berberine, Tetrandrine, Baicalin, Baicalein, Chrysin, Paeoniflorin.[30,31]

HED Alleviated TNBS-Induced Experimental Colitis

All Balb/c mice were sacrificed on day 6 after TBNS induction (Figure 2A). During the experiment, the TNBS group displayed typical clinical symptoms of UC relative to the CON group, comprising weight loss, diarrhea and macroscopic bloody stool (Figure 2B and C). Treatment with HED-L, HED-H, and SASP restored the weight loss in mice with colitis during disease progression (Figure 2C). Compared with the TNBS group, HED-L, HED-H and SASP groups enriched the survival rate of the colitis mice, due to death of two mice, the number of mice per group become eight instead of ten (Figure 2D). In terms of disease activity index (DAI) scores, the highest score was obtained on the first day after modeling and three drug intervention groups had significantly ($P \leq 0.05$ - $P \leq 0.001$) lower DAI score and inflammation than TNBS group (Figure 2E). TNBS induced intestinal wall thickening, edema, and ulcer formation in colitis mice (Figure 2F). Additionally, TNBS significantly ($P \leq 0.001$) increased colon weight and colon index (colon weight/length ratio), spleen weight and spleen index (spleen weight/body weight ratio) in the CON group. Treatment with HED-L, HED-H and SASP significantly ($P \leq 0.05$- $P \leq 0.0001$) alleviated TNBS-induced colonic edema and splenomegaly (Figure 2G–J), suggesting that HED has an anti-inflammatory effect on UC model mice.

Histological analysis manifested that the colonic mucosal epithelial cells in the CON group were intact, the structure of crypts was normal, the glands were tidily organized, and no atrophy, necrosis, inflammatory infiltration and other lesions were observed (Figure 2K). For the TNBS group, the severe epithelial cell injury showed less damage to glands, ulcers, and goblet cells, and severe inflammation accompanied by submucosal immune cell infiltration, leading to higher histological grades. Treatment with HED-L, HED-H and SASP, alleviated the degree of intestinal epithelial injury, markedly modified the number and area of ulcer lesions, substantially converted the infiltration of neutrophils and other immune cells.

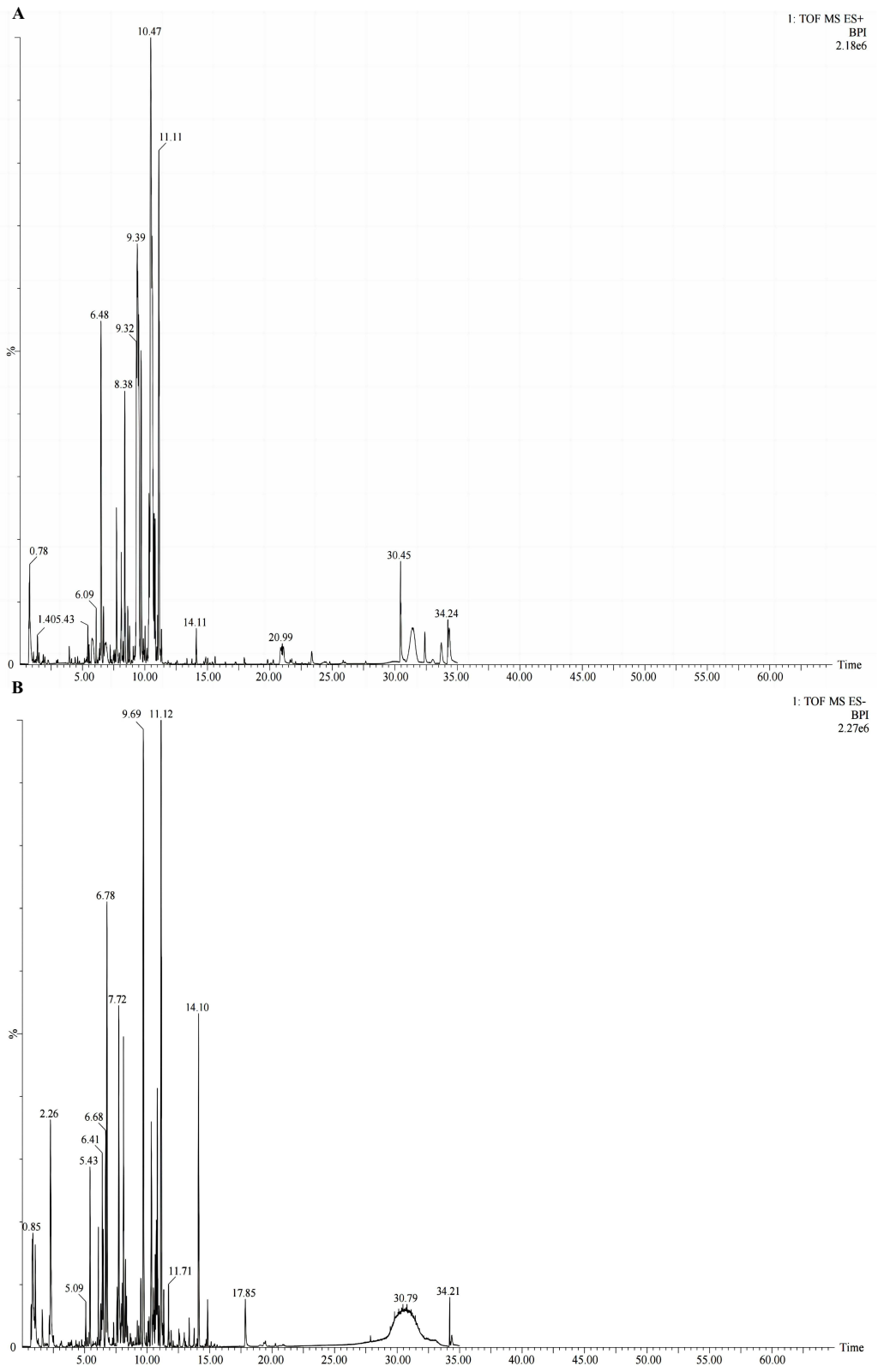

Figure 1 Representative base peak intensity (BPI) chromatograms of PNS in (**A**) positive and (**B**) negative modes. The numbering of identified compounds (1–58) is the same as in Table 1.

https://doi.org/10.2147/DDDT.S468608

https://doi.org/10.2147/DDDT.S468608

Table 3 Compounds Identified from HED by UPLC-Q-TOF/MS

NO.	T_R (min)	Identification	Molecular Formula	Theoretical Mass (Da)	$[M-H]^-$ / $[M+H]^+$(m/z)	Fragment Ions (Negative/Positive)	Source
1	0.85	D-(+)-Sorbose	C6H12O6	180.06	179.05	99.04, 145.05, 149.04/135.06, 145.04, 163.05	Baishao
2	2.27	Danshensu	C9H10O5	198.05	197.04/	135.04, 149.05, 151.03/	Huanglian
3	2.38	3-Carboxy-4-hydroxy-phenoxy glucoside	C13H16O9	316.07	315.07/	152.01, 230.01/	Huanglian
4	5.1	Tetrandrine	C38H42N2O6	622.30	/623.31	/596.29, 609.30	Huanglian
5	5.36	Cosmetin	C21H20O10	432.11	433.11	293.04, 311.05, 341.06/337.06, 379.08, 397.09	Huanglian
6	5.43	Cis-Ferulic acid	C10H10O4	194.06	193.05/	134.03, 149.05, 179.03/	Huanglian
7	5.46	Neochlorogenic acid	C16H18O9	354.09	353.09/	173.04, 179.03, 193.04/	Huanglian
8	5.88	Darendoside B	C21H32O12	476.18	475.18/	343.13, 387.12, 459.18/	Huanglian
9	6.1	Daidzin	C21H20O9	416.11	417.11	339.08, 379.08, 397.09/297.07, 341.09, 381.09, 399.10	Huanglian
10	6.1	1-O-β-D-Glucopyranosylpaeonisuffrone	C16H24O9	360.14	399.11	379.08, 337.07/281.08, 367.08, 449.14	Baishao
11	6.13	4-O-Galloylalbiflorin	C30H32O15	632.17	/631.16	/383.11, 415.10, 513.15, 574.12	Baishao
12	6.35	Hormothamnione	C21H20O8	400.11	445.11/	331.07, 355.08, 383.07/	Huangqin
13	6.42	2-Carboxymethyl-3-phenyl-2,3-epoxy-1,4-naphthoquinone	C17H16O5	300.09	/301.1	/197.09, 198.08	Huanglian
14	6.42	Paeonilactone-B	C10H12O4	196.07	/197.08	/109.06, 133.06, 151.07	Baishao
15	6.42	Paeonilactone-C	C17H18O6	318.11	/319.11	/179.07, 197.09, 301.10	Baishao
16	6.79	Albiflorin R1	C23H28O11	480.16	/503.15	/301.10, 463.16	Baishao
17	6.79	Lactiflorin	C23H26O10	462.15	463.16	309.09, 366.09, 479.15/323.11, 338.10	Baishao
18	6.79	Oxypaeoniflorin	C23H28O12	496.16	495.15/	405.15, 479.15, 508.15/	Baishao
19	6.79	Paeonoside	C15H20O8	328.12	327.11/	309.09, 445.11, 449.14/	Baishao
20	7.63	Eugeniin	C41H30O26	938.10	/977.06	/441.10, 751.04386	Baishao
21	7.7	Albiflorin	C23H28O11	480.16	525.16/	255.06, 297.07, 417.11/	Baishao
22	7.73	Paeonin C	C17H24O9	372.14	/411.10	/219.07, 289.07	Baishao

23	7.77	Berlambine	C20H17NO5	351.11	/352.11	/325.07, 295.06	Huanglian
24	8.01	1,2,3,4,6-Pentagalloylglucose	C41H32O26	940.11	/941.12	/731.11, 743.11	Baishao
25	8.02	Galloylpaeoniflorin	C30H32O15	632.17	631.16/	491.11, 583.14, 613.15/	Baishao
26	8.11	8-Debenzoylpaeonidanin	C17H26O10	390.15	/429.11	/322.10, 336.12	Baishao
27	8.78	Jatrorrhizine	C20H20NO4	338.13	/339.14	/306.11, 323.11	Huanglian
28	9.06	Paeoniflorin	C23H28O11	480.16	525.16/	338.10, 403.14, 463.15/	Baishao
29	9.07	1-O-beta-D-Glucopyranosyl-8-O-benzoylpaeonisuffrone	C23H28O10	464.16	509.16/	283.08, 338.10, 403.14/	Baishao
30	9.12	5,7,4′-Trihydroxy-8-methoxyflavanone	C16H14O6	302.07	/303.08	/271.05	Huangqin
31	9.33	Groenlandicine	C19H16NO4	322.10	323.11	275.05, 293.06, 306.07/279.08, 308.09	Huanglian
32	9.37	Moupinamide	C18H19NO4	313.13	/336.12	/174.04, 178.06, 279.08	Huanglian
33	9.5	(R)-Canadine	C20H21NO4	339.14	338.13/	309.09, 323.11/	Huanglian
34	9.7	Baicalin	C21H18O11	446.08	447.09	269.04, 311.05, 341.06, 383.07/269.04, 271.05, 417.11	Huangqin
35	9.7	Baicalein	C15H10O5	270.05	/271.05	/253.04	Huangqin
36	9.7	Norwogonin	C15H10O5	270.05	269.04/	192.01, 251.03/	Huangqin
37	9.79	Viscidulin II	C17H14O7	330.07	331.08	299.01, 314.04/301.03, 316.056	Huangqin
38	10.15	Dihydrobaicalein	C15H12O5	272.06	273.07	271.05, 371.11/169.01	Huangqin
39	10.15	Dihydrobaicalin	C21H20O11	448.10	449.10	313.07, 371.11/253.04, 269.04,271.05	Huangqin
40	10.45	Berberine	C20H18NO4	336.12	/337.12	/276.06, 290.08, 309.13	Huanglian
41	10.46	Javanicin	C15H14O6	290.07	/291.08	/222.08, 250.08, 274.08	Huangqin
42	10.47	Salidroside	C14H20O7	300.12	323.11	121.06, 165.05, 233.08/232.07, 236.11, 251.08	Huangqin
43	10.47	Berberrubine	C19H15NO4	321.10	322.10	292.09, 304.09, 309.09/276.06, 294.11	Huanglian
44	10.47	2-(4-Morpholinyl)-8-phenyl-4H-1-benzopyran-4-one	C19H17NO3	307.12	/308.12	/275.09, 279.12	Huangqin
45	10.47	Paeonilactone A	C10H14O4	198.08	/221.07	/179.06, 169.01	Baishao

(*Continued*)

https://doi.org/10.2147/DDDTS468608

https://doi.org/10.2147/DDDT.S468608

Table 3 (Continued).

NO.	T_R (min)	Identification	Molecular Formula	Theoretical Mass (Da)	$[M-H]^-$ / $[M+H]^+$(m/z)	Fragment Ions (Negative/Positive)	Source
46	10.51	Scutevulin	C16H12O6	300.06	/301.06	/286.04	Huangqin
47	10.51	5,8,2′-Trihydroxy-7-methoxyflavone	C16H12O6	300.06	299.05/	267.02, 284.03/	Huangqin
48	10.56	Isomartynoside	C31H40O15	652.23	651.23/	426.11, 461.11, 487.16/	Huangqin
49	10.57	Coptisine	C19H14NO4	320.09	/321.09	/290.08, 304.09	Huanglian
50	10.71	Chrysin	C15H10O4	254.05	255.06	151.00, 237.05/239.06	Huangqin
51	11.12	Wogonin	C16H12O5	284.06	285.07	240.04, 268.03/241.04, 270.05	Huangqin
52	11.12	Oroxindin	C22H20O11	460.10	461.10	283.06, 293.04, 441.08/269.04, 285.07	Huangqin
53	11.33	5,8-Dihydroxy-6,7-dimethoxyflavone	C17H14O6	314.07	315.08	283.02,298.04/183.02, 285.03	Huangqin
54	11.35	Dihydrooroxylin	C16H14O5	286.08	287.09	229.04, 253.04, 271.05/183.02, 254.05686	Huangqin
55	14.12	3beta,23-Dihydroxyoleana-11,13(18)-dien-28-oic acid	C30H46O4	470.33	/471.34	/285.22, 435.32, 453.33	Baishao
56	15.18	Neobaicalein	C19H18O8	374.10	/375.10	/345.05	Huangqin
57	15.18	Skullcapflavone II	C19H18O8	374.10	373.09/	328.02, 358.06, 343.04/	Huangqin
58	31.98	Magnograndiolide	C15H22O4	266.15	265.14	233.15, 249.11/235.09	Huangqin

Notes: *Only three components of Coptidis Rhizoma, Radix scutellariae and White peony root were identified. *The mass spectrometry is used for qualitative detection of traditional Chinese medicine, and what is measured is the relative mass number.

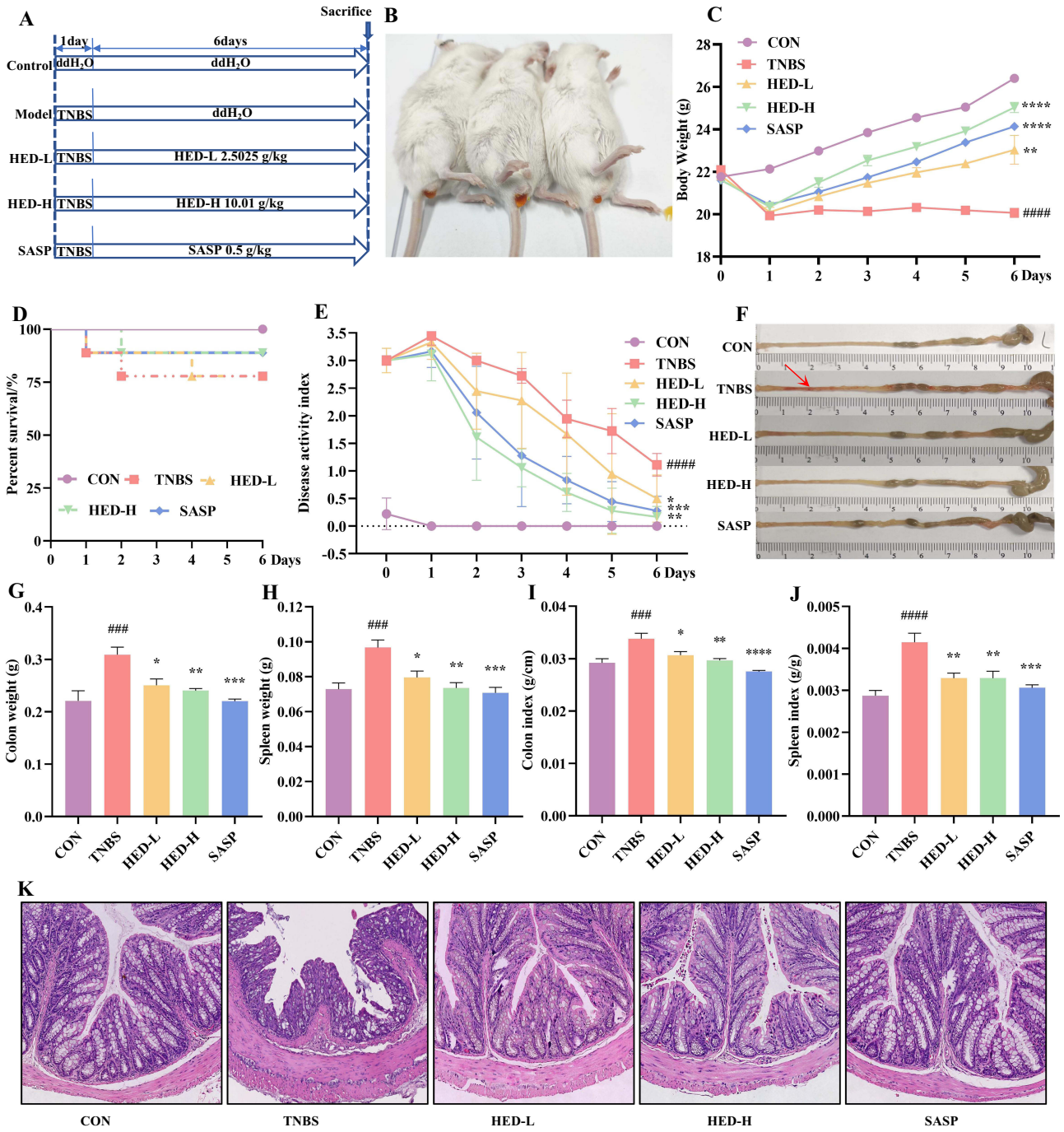

Figure 2 HED treatment mitigated TNBS-induced UC in mice. (**A**) Experimental design; (**B**) Modeling of Balb/c colitis mice; (**C**) Body weight of mice; (**D**) Survival rate in TNBS-induced ulcerative colitis in mice; (**E**) DAI score; (**F**) Image of the colon (arrows indicating the injury sites); (**G**) Colon weight; (**H**) Spleen Weight; (**I**) Colonic index; (**J**) Spleen index; (**K**) Representative H&E-stained colon sections (40× magnification, cross-sectional images of the colon selected at random). Data were shown as mean ± SEM (n=6): $^{\#\#\#\#}P < 0.001$, $^{\#\#\#\#\#}P < 0.001$, compared to the CON group; $^{*}P < 0.05$, $^{**}P < 0.01$, $^{***}P < 0.001$, $^{****}P < 0.001$, compared to the TNBS group.

Transcriptomic Effects of HED-H on TNBS-Induced Colitis

Following a rigorous evaluation based on the above provided data, colon of the HED-H group was chosen for transcriptome sequencing due to its demonstrably greater improvement over HED-L. To profoundly explore the underlying mechanisms of HED-H in the treatment of colitis mice, we adopted a transcriptome sequencing using the colon tissues. Volcano graphs were prepared for demonstrating DEGs in TNBS VS CON and HED-H VS TNBS (Figure 3A–B). As for the CON group, 682 genes were downregulated and 482 genes were upregulated in the TNBS group. In the TNBS group 773 genes were downregulated

https://doi.org/10.2147/DDDT.S468608

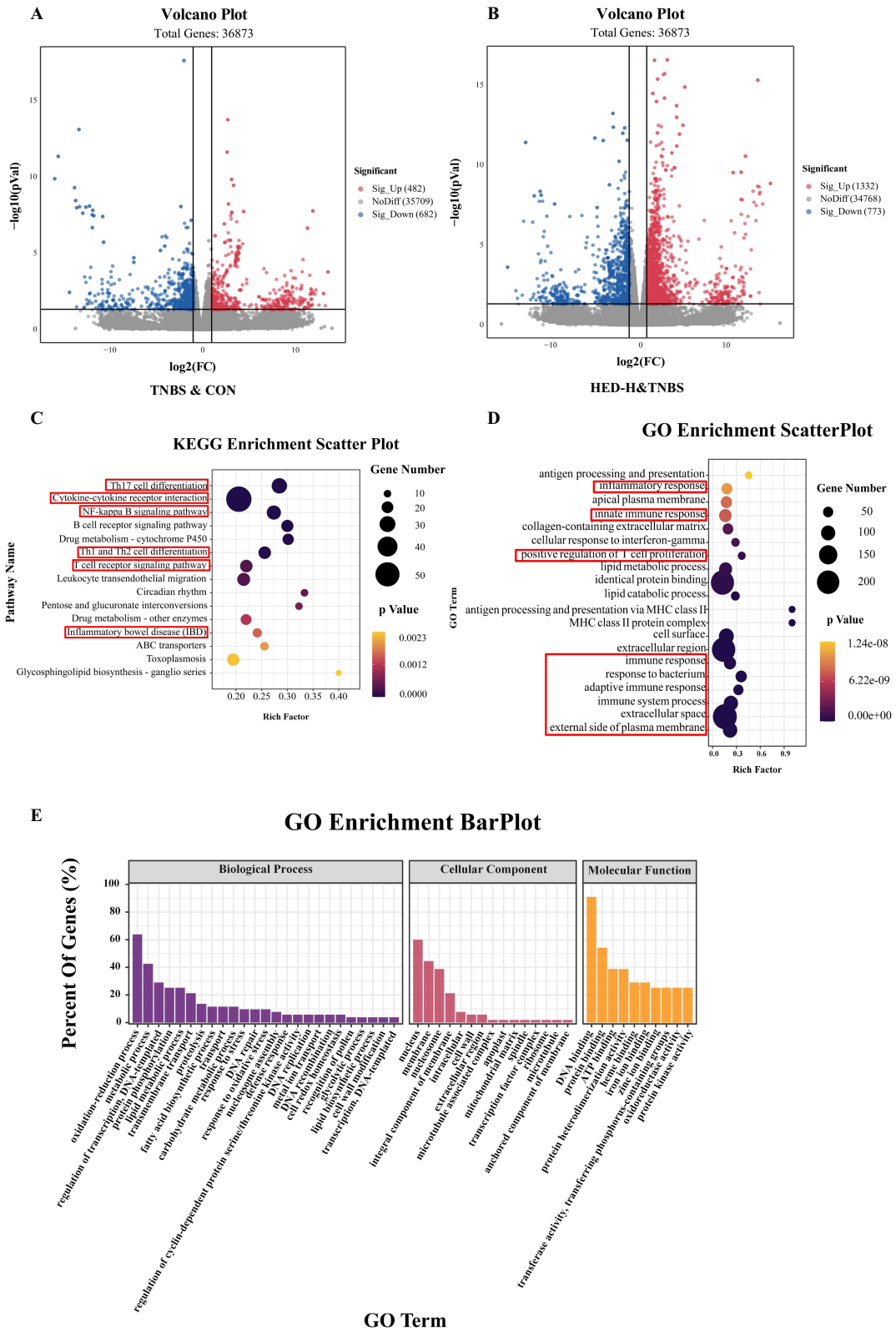

Figure 3 Colon transcriptome analyzed by RNA sequencing (n=3). (**A**) Volcano plot demonstrating the DEGs in the TNBS and CON groups. The red dots indicate the upregulated genes, the blue dots show the downregulated genes, and the grey dots indicate genes with no significant change; (**B**) Volcano plot showing the DEGs in the HED-H and TNBS groups; (**C**) KEGG pathway enrichment analysis; (**D**) GO pathway enrichment analysis; (**E**) Specific BP, CC, and MF are shown in barplot; Deep red bars represent MF terms. Light red bars represent CC terms. Light yellow bars represent BP (n=3).

https://doi.org/10.2147/DDDT.S468608

and 1332 genes upregulated after treatment with HED-H. As analyzed in KEGG, with reference to the results of P-values, the majority of DEGs were distinctly enriched in the T cell-related pathways (Th17 cell differentiation, Th1 and Th2 cell differentiation and T cell receptor signaling), NF-kappa B signaling pathway and cytokine–cytokine receptor interaction (Figure 3C). GO enrichment BarPlot results indicated that the DEGs mainly participated in T cell proliferation, inflammatory response, immune response, response to bacterium and extracellular space, eg(Figure 3D). The top 25, 15, and 10 most meaningful GO terms in biological processes (BP), cellular component (CC), and molecular function (MF) were oxidation-reduction process, metabolic process, and regulation of transcription in BP; nucleus, membrane, nucleosome and integral component of membrane in CC; DNA bonding, protein bonding and ATP bonding in MF (Figure 3E). Through KEGG and GO analysis, the anti-inflammatory mechanism of HED-H in UC could be related to $CD4^+$T cell subsets (Th1/Th2/Th17) and gut microbiota.

HED Restored Th2/Th1 and Th17/Treg Cells Balance in the Colon of TNBS-Induced Colitis Mice

The dynamic balance between $CD4^+$T cell subsets plays a crucial portion in the deformation and occurrence of UC.[32] To explore whether HED could induce anti-inflammatory mechanism in UC model mice, we applied flow cytometry to analysis $CD4^+$T cell subsets (Th1, Th2, Th17, Tregs). Then, we ascertained the effect of HED on the balance of regulatory $CD4^+$T cell subsets in TNBS-induced UC by measuring the percentages of Th1, Th2, Th17 and Tregs in colonic tissue by flow cytometry (Figure 4A). The percentage of CD4, Th1 and Th2 cells in the TNBS group were significantly ($P \leq 0.01$-$P \leq 0.0001$) increased compared to the CON group. In the 3 treated groups, the HED-L and SASP groups had a significant recovery of CD4, Th1 and Th2 cell proportions (Figure 4B-D). The HED-L group significantly ($P \leq 0.01$-$P \leq 0.001$) restored the percentage of Th1 and Th2 cells, but did not restore the percentage of CD4+ cells, compared with the TNBS group (Figure 4B–D). The percentage of Th17 and Tregs showed no statistically significant difference in all groups, except for the percentage of Th17 in the SASP group (Figure 4E–F). The Th2/Th1 ratio was significantly ($P \leq 0.01$) increased in the TNBS group, while it was significantly ($P \leq 0.01$) reduced in HED-H and SASP (Figure 4G). In the TNBS group, Tregs/Th17 ratio was also significantly ($P \leq 0.01$) decreased, while in the 3 treated groups this ratio was significantly ($P \leq 0.01$) recovered to a limit comparable to the CON group (Figure 4H).

HED Shifted the TNBS-Induced UC Mice Th2/Th1 and of Tregs/Th17 Related Cytokines

We initially assessed the protein and mRNA expression of T-bet and Gata3 in colon tissues. As compared to the CON group, T-bet and Gata3 gene and protein expression was significantly ($P \leq 0.01$- $P \leq 0.001$) elevated in the TNBS group, which were ($P \leq 0.05$- $P \leq 0.001$) reduced towards normal levels by treatment with HED-L, HED-H and SASP (Figures 5A and 6A).

The TNBS group exhibited significantly ($P \leq 0.01$- $P \leq 0.0001$) higher expression of IL-4 and IL-6 genes/proteins compared to the CON group, and this expression was significantly ($P \leq 0.05$- $P \leq 0.0001$) downregulated in the HED-L, HED-H and SASP groups (Figures 5B and 6B). In the TNBS group, there was a significant ($P \leq 0.0001$- $P \leq 0.0001$) decrease in the expression of IL-10 and a significant ($P \leq 0.001$ - $P \leq 0.0001$) increase in the expression of both IL-1β and IL-17A genes/proteins. Moreover, treatment with HED-L, HED-H and SASP effectively mitigated these inflammatory changes towards normalization, which was a significant ($P \leq 0.05$- $P \leq 0.001$) increase in the expression of IL-10 and a significant ($P \leq 0.05$ - $P \leq 0.001$) decrease in the expression of both IL-1β and IL-17A genes/proteins (Figures 5C and 6C).

HED Enhanced Intestinal Barrier Function of TNBS-Induced UC

The close relationship between T cells and intestinal barrier function prompted us to ulteriorly investigate the influence of HED on intestinal barrier function. Tight junction protein Occludin and ZO-1 were chosen to assess HED treatment effects on UC intestinal barrier function. Western blot and qPCR results revealed that the expression of Occludin and ZO-1 tight junction proteins/genes were significantly ($P \leq 0.0001$) declined in the TNBS group, while treatment with HED-L, HED-H or SASP significantly ($P \leq 0.05$- $P \leq 0.001$) elevated this expression. These results infer that HED and SASP therapy can restore bowel barrier function in UC mice (Figures 5D and 6D).

https://doi.org/10.2147/DDDT.S468608

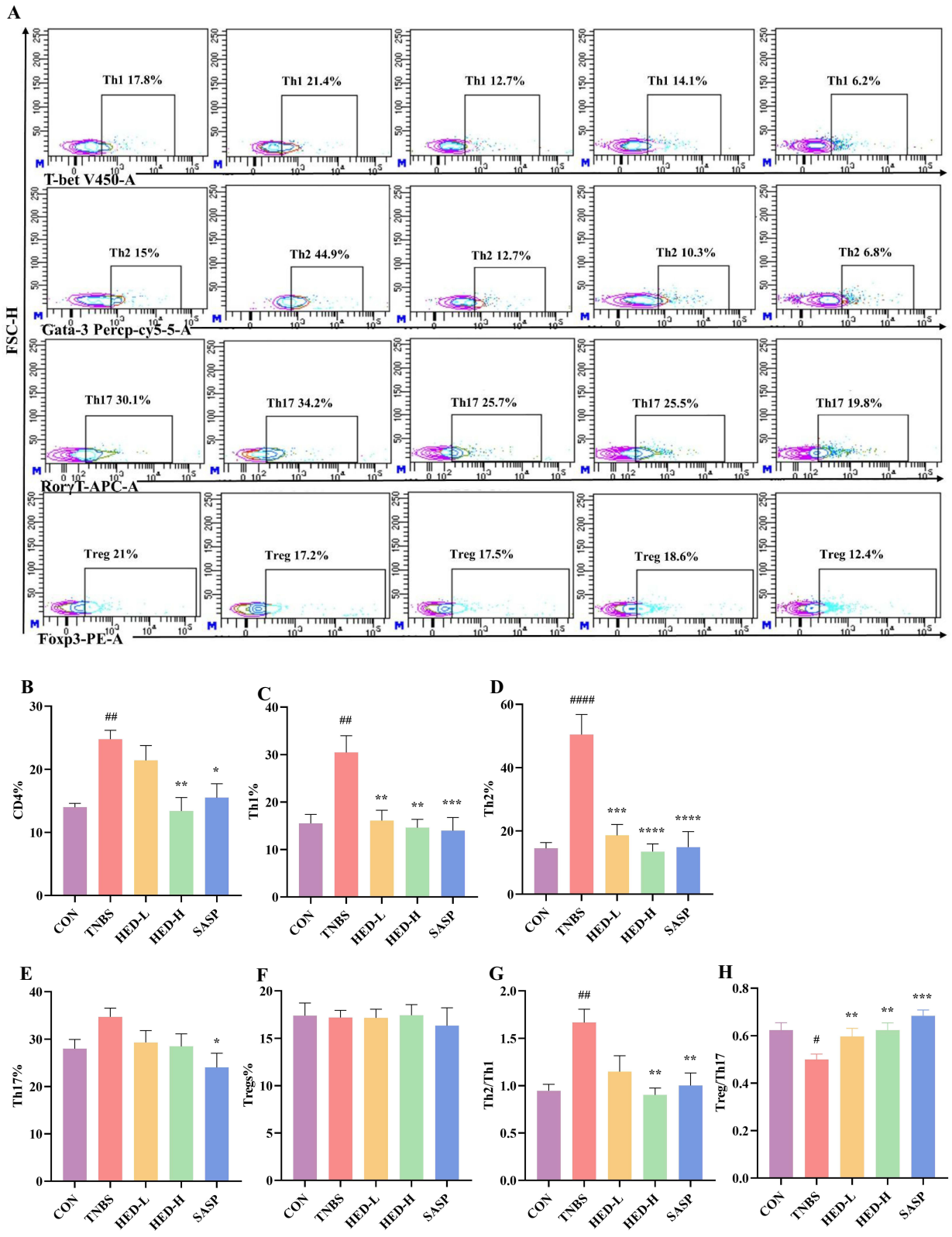

Figure 4 HED treatment restored the balance of Th2/Th1 and Tregs/Th17 cells in the colon tissue of TNBS-induced colitis mice. (**A**) Percentage of Th1, Th2, Th17, and Treg cells; (**B-F**) Statistics of the proportion of CD4, Th1, Th2, Th17, and Treg cells; (**G-H**) The ratio of Th2/Th1 and Tregs/Th17 cells; Data were shown as mean ± SEM (n=6): $^{\#}P < 0.05$, $^{\#\#}P < 0.01$, $^{\#\#\#\#}P < 0.001$, compared to the CON group; $^{*}P < 0.05$, $^{**}P < 0.01$, $^{***}P < 0.001$, $^{****}P < 0.001$, compared to the TNBS group.

https://doi.org/10.2147/DDDT.S468608

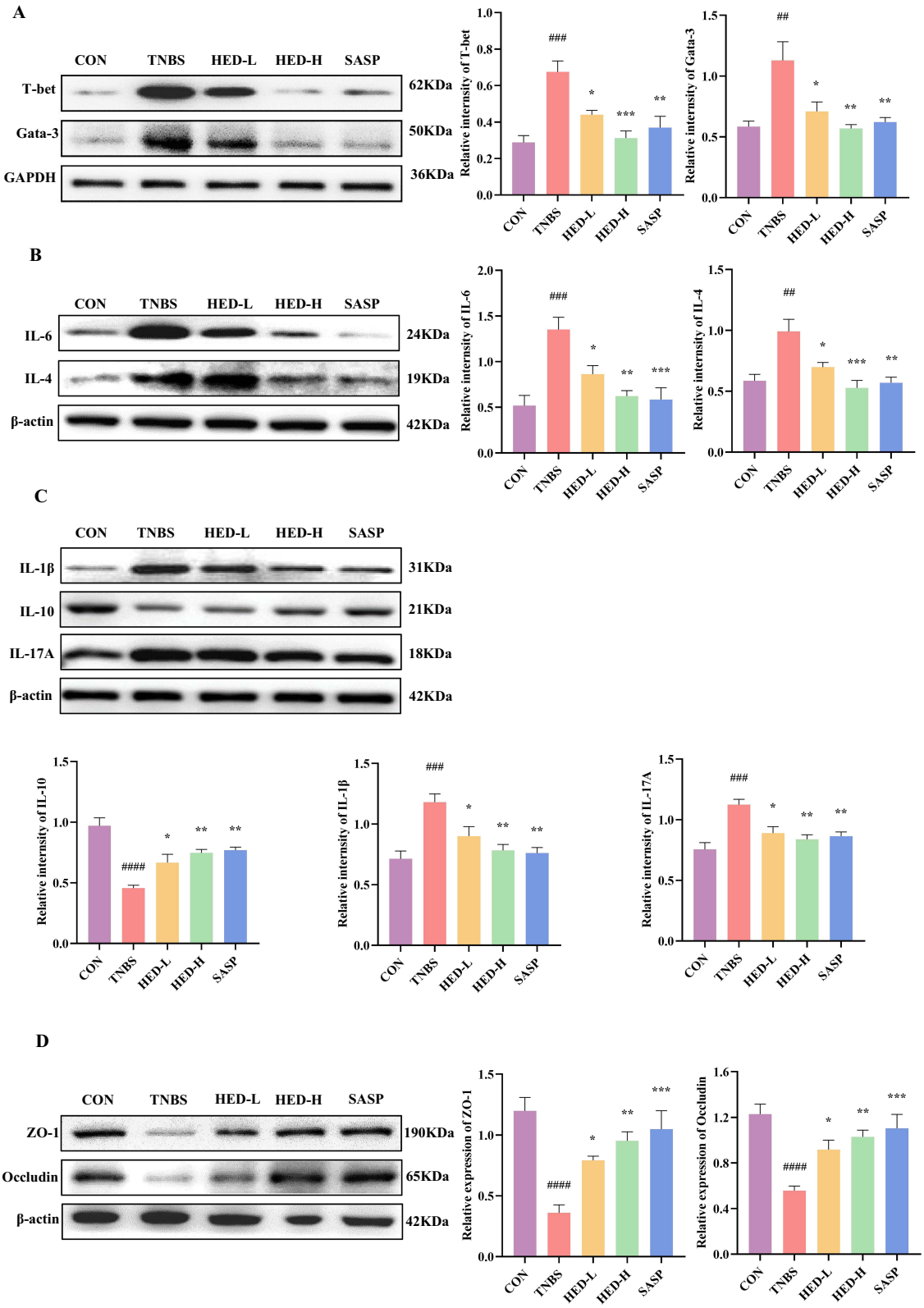

Figure 5 Western blot for (**A**) T-bet and Gata-3; (**B**) IL-6 and IL-4; (**C**) IL-1β, IL-10 and IL-17A; (**D**) Zo-1 and Occludin; Data were presented as mean ± SEM (n=5): $^{\#\#}P < 0.01$, $^{\#\#\#}P < 0.001$, $^{\#\#\#\#}P < 0.001$, compared to the CON group; $^{*}P < 0.05$, $^{**}P < 0.01$, $^{***}P < 0.001$, compared to the TNBS group.

https://doi.org/10.2147/DDDT.S468608

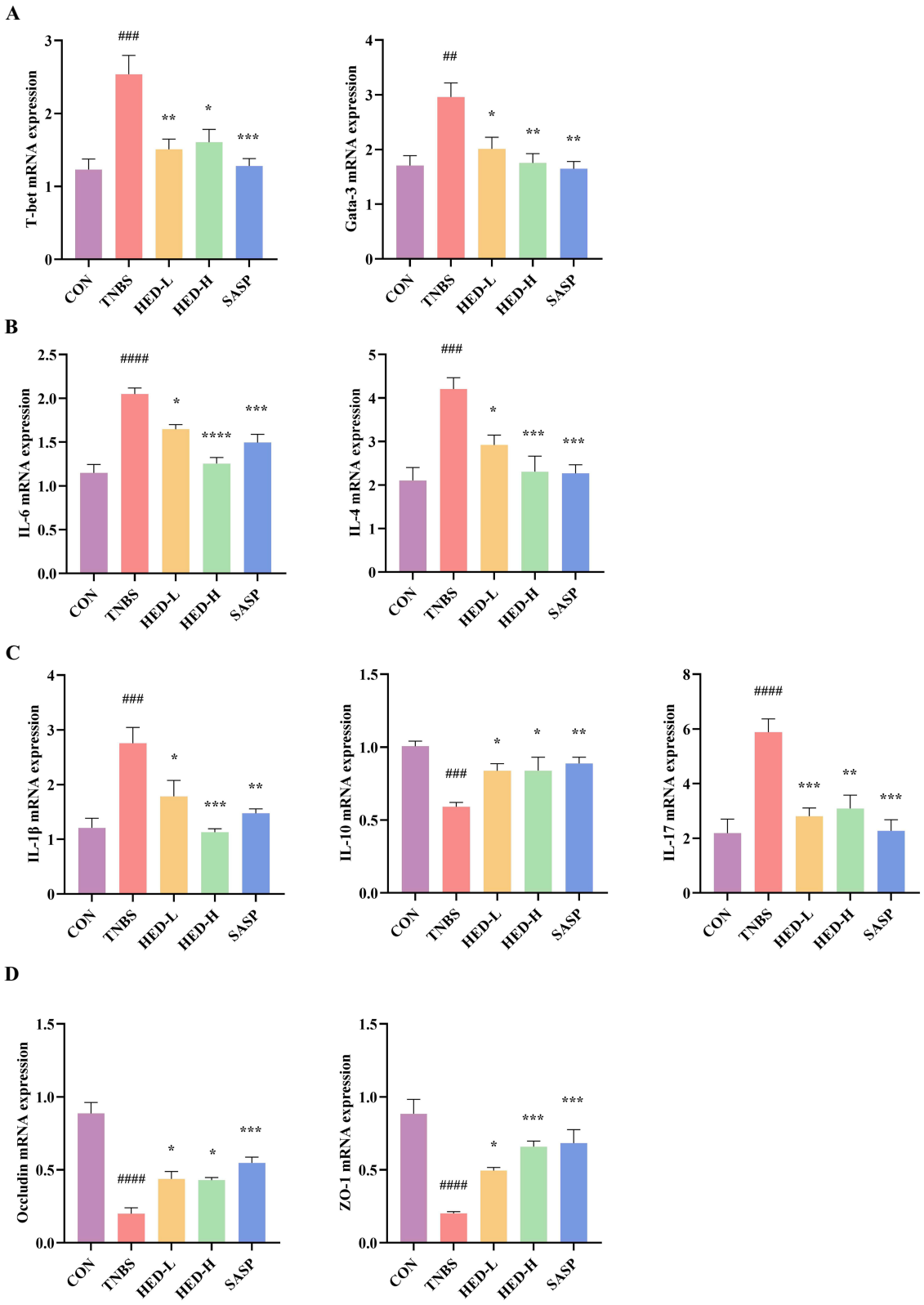

Figure 6 Relative mRNA expression of (**A**) T-bet and Gata-3; (**B**) IL-6 and IL-4; (**C**) IL-1β, IL-10 and IL-17; (**D**) Zo-1 and Occludin; Data were presented as mean ± SEM (n=5): $^{\#\#}P < 0.01$, $^{\#\#\#\#}P < 0.001$, $^{\#\#\#\#\#}P < 0.001$, compared to the CON group; *P < 0.05, **$P < 0.01$, ***$P < 0.001$, ****$P < 0.001$, compared to the TNBS group.

https://doi.org/10.2147/DDDT.S468608

HED Treatment Significantly Altered the Gut Microbiota in TNBS-Induced Colitis Mice

To determine whether the HED treatment altered the microflora, we performed high-throughput genetic sequencing of 16Sr DNA in the faecal bacterial DNA of the CON, TNBS and HED-H groups. As shown in Figure 7A–B, the occurrence of Chao1 and Shannon indices representing α-diversity of the intestinal ecosystem were markedly different among the three groups,

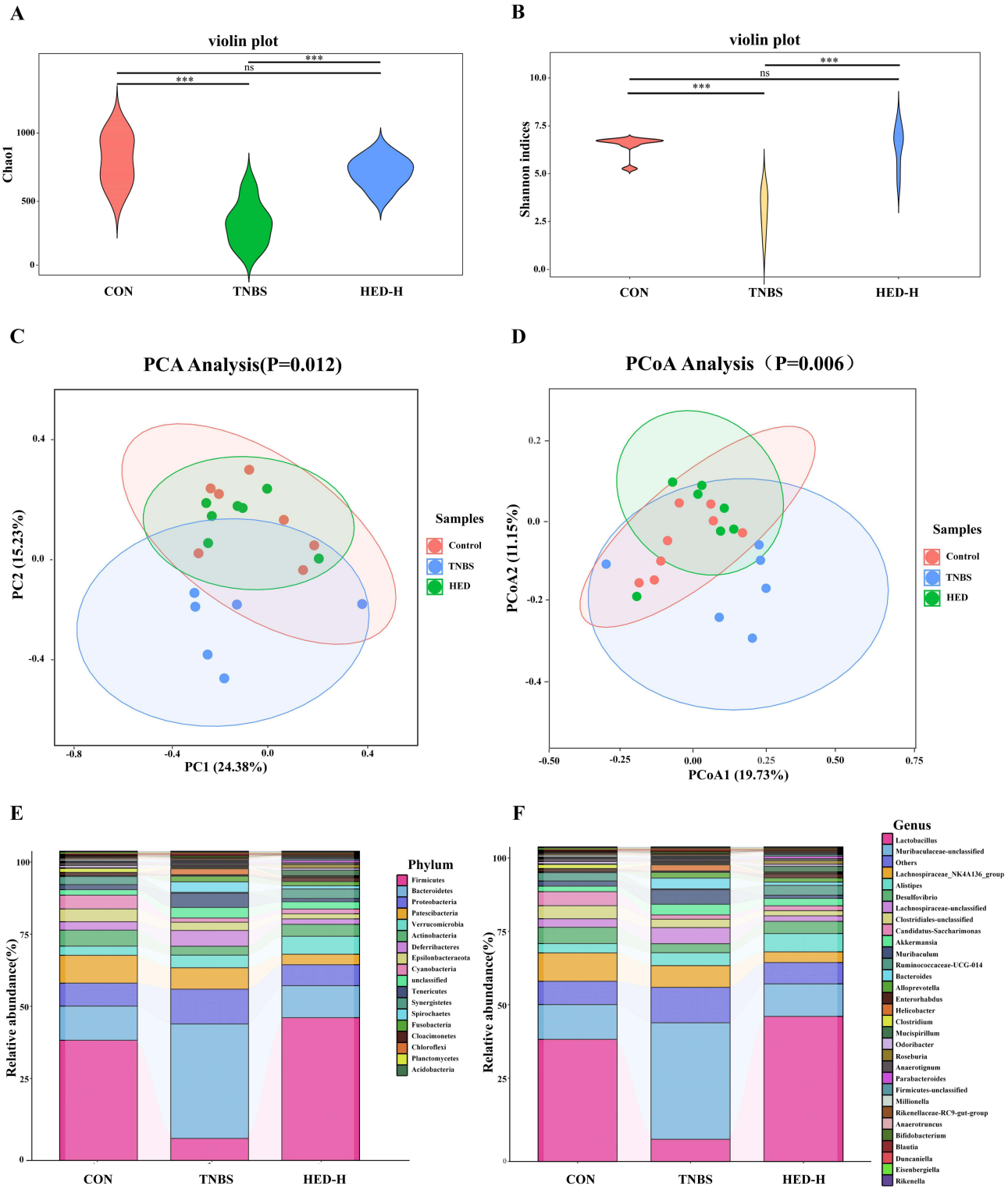

Figure 7 Continued.

https://doi.org/10.2147/DDDT.S468608

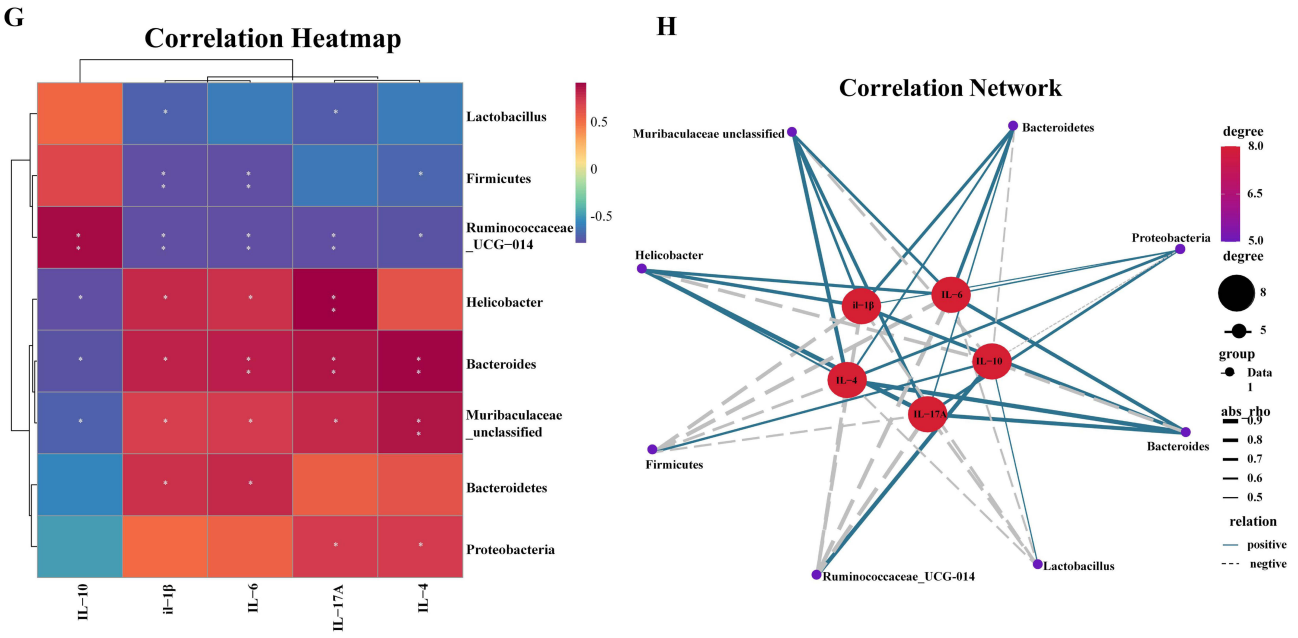

Figure 7 HED-H altered the gut microbiota in TNBS-induced colitis mice. (**A-B**) The results of α-diversity analysis containing Chao1 and Shannon among CON, TNBS and HED-H groups; (**C-D**) The results of β-Diversity analysis including PCA and PCoA in different groups; (**E-F**) Community bar plot analysis of gut microbiota at the phylum level and genus level; (**G-H**) Gut microbiota and inflammatory cytokines were shown with Correlation Heatmap and Correlation Network between (n=3): $^{\#\#\#}P < 0.001$, compared to the CON group; $^{***}P < 0.001$, compared to the TNBS group; ns indicated no significant ($P > 0.05$).

both indices were massively down-regulated in the TNBS group relative to the CON, while both indices were reinstated after HED-H intervention. Additionally, β-diversity analysis such as Principal coordinate analysis (PCoA) and the differences of principal component analysis (PCA) were also performed among the groups (Figure 7C-D). The strain repetition rate was higher in HED-H group and CON group, especially in PCA. The results showed that UC mice colonies gradually returned to normal after the HED-H intervention. Based on the results of the α-diversity and β-diversity analysis described above, we suggest that HED could restore microbial community diversity in TNBS-induced colitis mice to some extent.

In the microbial diversity analysis of cluster analysis, we have shown the results of flora richness at the phylum and genus levels, where phylum includes Firmicutes, Bacteroidetes and Proteobacteria and genus level contains Lactobacillus, Muribaculaceae_unclassified, Ruminococcaceae_UCG-014, Bacteroides and Helicobacter pylori, the seven colonies mentioned above showed that exhibited prominent differences of the relative abundance between the TNBS and CON groups. Their relative abundances were enormously reversed by HED-H (Figure 7E–G).

To further investigate the relationship between gut microbiota and inflammation, we analyzed the strains and inflammatory factors that showed significant differences in the experiment by drawing heat maps. Most of the inflammatory factors such IL-Iβ, IL-6, IL-17AA and strains were closely related, as indicated by the correlation diagram (Figure 7H), in which Muribaculaceae_unclassified, Bacteroidetes and Ruminococcaceae_UCG-014 were significantly different from all inflammatory factors, manifesting that these bacteria groups play an influential regulatory assignment in the anti-inflammatory effects of observed in the HED-H group.

Discussion

Traditional Chinese medicine (TCM) plays a crucial role as one of the effective treatments for UC, especially for the remission and recurrence of the clinical symptoms of UC.[33] The discovery and exploration of effective TCM prescriptions for the treatment of UC have been progressing. Of these, TCM, Gegen Qinlian Decoction, Peony Decoction, Licorice Xiexin Decoction were reported to play a significant anti-inflammatory effect in the treatment of UC animal model.[13,34–37] HED is one of the classic prescriptions of TCM In our current study, HED was shown to be effective against UC and to improve survival in TNBS-induced colitis mice. Moreover, UC mice recovered significantly after HED treatment in terms of body weight, DAI score, colon weight and index, spleen weight and index, and pathological score.

In order to further probe into the potential mechanism of HED anti-UC, we conducted research from two aspects. On the one hand, transcriptional sequencing KEGG and GO analysis showed that HED could positively affect $CD4^+$T cell subsets (Th1, Th2 and Th17) and gut microbiota. On the other hand, the main components of HED decoction, such as Berberine, Tetrandrine, Baicalin, Baicalein, Chrysin, Paeoniflorin, eg. were identified as monomers to exert anti-UC effects by regulating $CD4^+$T cells and gut microbiota.[38–43] Therefore, we hypothesized that the HED mechanism could involve CD4 subsets and gut microbiota, which were further validated by us using flow cytometry, WB, and 16s sequencing.

The imbalance between CD4 subsets, especially Th1, Th2, Th17, and Tregs, leads to progressive and recurrent episodes of UC.[32] The latter was previously defined as a disease dominated by atypical Th2 elevation.[44] It has been reported in the literature that TNBS can cause disorders of Th1, Th2 and Th17.[45] So we used TNBS to induce Balb/c mice and established a model with significantly elevated Th2 ratio. Flow cytometry results revealed that the proportion of Th1, Th2 and Th17 increased in the TNBS group, especially the proportion of Th2, which was most significantly increased. Contrarily, HED treatment reversed this trend, specifically inhibiting the increase in Th2 and Th1 ratios. GATA3 and T-bet are key transcription factors of Th2 and Th1, which facilitate the differentiation of Th1 and Th2.[46] The protein and mRNA of GATA3 and T-bet in the TNBS group were highly expressed, while treatment with HED significantly reduced the levels of GATA3 and T-bet in a dose-dependent manner, which indicates that HED could weaken the activity of Th1 and Th2 cells by reducing the expression levels of GATA3 and T-bet. Additionally, high dose HED could also significantly restore higher Th2/Th1 and lower Treg/17 ratio in UC mice. Taken together, HED could exert anti-inflammatory effects by regulating the balance of Th2/Th1 and Treg/Th17, mainly through the inhibition of the Th2 /Th1 ratio.

Previous studies reported that the overexpression of specific pro-inflammatory factors such as IL-6, IL-1β and IL17 in UC patients could induce intestinal mucosal inflammation and damage, while the inhibition of the anti-inflammatory factor IL-10 could aggravate the inflammatory response of UC.[46] Subsequently, we evaluated $CD4^+$T subgroup-related cytokines (IL-4, IL-6, IL-17A, IL-10, and IL-1β), and found remarkable changes in these markers. Of interest, HED therapy reversed the increase in IL-6 and IL-17A and the decrease in IL-10 in the TNBS group. IL-4 fosters undifferentiated $CD4^+$T cells into Th2 subsets and activates Th2 cells, which can activate Th2 cells, inhibit Th1 cells, and maintain the balance between Th1 and Th2.[47] Overexpression of IL-4 may lead to immune disorders and the persistence of intestinal inflammation, which has a negative impact on the treatment and prognosis of UC.[48] Our results showed that the expression of IL4 was vastly increased in UC mice, while this expression was decreased after HED treatment. This result indicated that HED could reduce inflammation by decreasing IL-4, thereby inhibiting the differentiation of Th2 and Th1.

Accumulating evidence has established that intestinal flora is one of the essential pathogenesis mechanisms of UC.[33] The imbalance of gut microbiota causes immune disorders, accompanied by impaired intestinal barrier function and continuous inflammatory response, resulting in the progression of UC.[49] In this present study, we substantiated that the intestinal microbial composition of UC mice treated with HED not only changed significantly, but also the microbiota diversity was restored, revealing that the phylactic effect of HED on TNBS-induced UC may be correlated with the intestinal microbial population. In agreement with previous DSS model studies, at the phylum level, relative abundances of Firmicutes increased overwhelmingly and Bacteroidetes decreased tremendously after TNBS treatment relative to the CON group. In UC patients, a similar microbiota dysbiosis was observed, with a decreased ratio of Firmicutes to Bacteroidetes (F/B).[50] The phylum Proteobacteria was found to be the predominant group in the intestinal microbiota of the normal control mice, enormously increased in TNBS group, while HED treatment restored the changes in Proteobacteria, Firmicutes and Bacteroides.[51]

At the genus level, HED impaired the effect of TNBS on beneficial bacterial genera in the gut. Lactobacillus and Bacteroides were shown to beef up intestinal barrier function through the promotion of TJ protein expression in intestinal epithelial cells, reduction of apoptosis in epithelial cells, and modulation of the intestinal mucus layer.[52] Ruminococcaceae_UCG-014 is closely related to the production of butyrate, a major energy source of intestinal epithelial cells, and also inhibits the signaling pathway for pro-inflammatory cytokines. In addition, its abundance leads to increased mucin secretion and tight junctions, thereby enhancing intestinal barrier function. The abundance of these three bacteria after HED treatment suggests that improved intestinal barrier function in UC mice after HED treatment. In addition to the above three obvious flora, there is Akkermansia muciniphila, as an important microorganism in the intestinal flora, which can provide energy for intestinal cells by degrading mucin and promote the release of intestinal mucin, thereby enhancing the integrity of the intestinal mucosal barrier.[53] In support, HED treatment reversed the decline in intestinal barrier function, as

evidenced by the expression of key tight junction proteins ZO-1 and occludin in the TNBS group. Levels of these crucial proteins/genes returned to near normalcy, mirroring those observed in the healthy control group.[54,55] Notably, Helicobacter pylori (*H. pylori*), as an opportunistic pathogen, is highly associated with inflammation of the gut and is commonly significantly increased after induction of the DSS model. Similarly, we found that *H. pylori* abundance increased significantly after TNBS induction and decreased significantly after HED treatment, suggesting that HED may reduce the pathogen content to alleviate colitis. These results demonstrated that the variation in the levels of these bacteria may have predominantly contributed to the anti-UC effects of HED. Interactions between gut microbiota and cytokines are complex and bidirectional.[56] With HED regulation of cytokines and key flora, correlation heatmaps and network results were drawn to show that most flora and cytokines are closely related, reflecting that flora and $CD4^+$T are indispensable components of the HED anti-inflammatory mechanism.[57]

The study validated the potential mechanisms of HED on TNBS-induced UC Balb/c mice. The regulation of Th2/Th1 and Tregs/Th17 cell balance, as well as the modulation of gut microbiota by HED and restoring intestinal barrier function providing more mechanistic basis for amelioration of UC.

Ethical Approval

All animal research protocols conducted in this study were authorized by the Animal Ethics Committee of Zhejiang Chinese Medical University (IACUC-20220307-22).

Acknowledgments

We appreciate the great help/technical support/experimental support from the Pharmaceutical Research Center, Academy of Chinese Medical Sciences, Zhejiang Chinese Medical University.

Author Contributions

All authors made a significant contribution to the work reported, whether that is in the conception, study design, execution, acquisition of data, analysis and interpretation, or in all these areas; took part in drafting, revising or critically reviewing the article; gave final approval of the version to be published; have agreed on the journal to which the article has been submitted; and agree to be accountable for all aspects of the work.

Funding

This research was funded by National Natural Science Foundation of China (No. 82274475); 2022 General Scientific Research Project of Zhejiang Provincial Department of Education-Special Project for Reform of Professional Degree Graduate Training Mode (No. Y202248721); 2022 Zhejiang Chinese Medicine University Postgraduate Scientific Research Fund Project (No. 2022YKJ06); Zhejiang Xinmiao Talents Program (No. 2022R410B048; No. 2023R410015).

Disclosure

The authors declare that there are no conflicts of interest in this work.

References

1. Katsandegwaza B, Horsnell W, Smith K. Inflammatory bowel disease: a review of pre-clinical murine models of human disease. *Int J Mol Sci*. 2022;23(16):19. doi:10.3390/ijms23169344
2. Mitsialis V, Wall S, Liu P, et al. Single-cell analyses of colon and blood reveal distinct immune cell signatures of ulcerative colitis. *Gastroenterology*. 2020;159(2):591–+. doi:10.1053/j.gastro.2020.04.074
3. Molina-Infante J, Rodríguez-Lago I. Modifying the natural history of gastrointestinal diseases in Europe as a result of early diagnosis: from eosinophilic esophagitis to inflammatory bowel disease. *United Eur Gastroenterol J*. 2022;10(7):612–613. doi:10.1002/ueg2.12256
4. Rubin DT, Ananthakrishnan AN, Siegel CA, et al. ACG clinical guideline: ulcerative colitis in adults. *Am J Gastroenterol*. 2019;114(3):384–413. doi:10.14309/ajg.0000000000000152
5. Turner D, Ricciuto A, Lewis A, et al. STRIDE-II: an update on the selecting therapeutic targets in inflammatory bowel disease (STRIDE) initiative of the international *gastroenterology. Gastroenterology*. 2021;160(5):1570–1583. doi:10.1053/j.gastro.2020.12.031
6. Saravia J, Chapman NM, Chi HB. Helper T cell differentiation. *Cell Mol Immunol*. 2019;16(7):634–643. doi:10.1038/s41423-019-0220-6
7. Mohebali N, Weigel M, Hain T, et al. Faecalibacterium prausnitzii, bacteroides faecis and roseburia intestinalis attenuate clinical symptoms of experimental colitis by regulating Treg/Th17 cell balance. *Biomed Pharmacother*. 2023;167:115568. doi:10.1016/j.biopha.2023.115568

8. Saba E, Lee YY, Rhee MH, et al. Alleviation of ulcerative colitis potentially through th1/th2 cytokine balance by a mixture of rg3-enriched Korean red ginseng Extract. *Molecules*. 2020;25(22):16. doi:10.3390/molecules25225230
9. He HP, Yang TH, Li F, et al. A novel study on the immunomodulatory effect of umbilical cord derived mesenchymal stem cells pretreated with traditional Chinese medicine Asarinin. *Int Immunopharmacol*. 2021;100:10. doi:10.1016/j.intimp.2021.108054
10. Gamah M, Alahdal M, Zhang Y, et al. High-altitude hypoxia exacerbates dextran sulfate sodium (DSS)-induced colitis by upregulating Th1 and Th17 lymphocytes. *Bioengineered*. 2021;12(1):7985–7994. doi:10.1080/21655979.2021.1975017
11. Wei W. Expert consensus on the diagnosis and treatment of ulcerative colitis with integrated traditional Chinese and western medicine. *J Integr Nurs*. 2023;5:1–7.doi:10.7661/j.cjim.20221027
12. Wei W, Wang Hua-hong YQ. Guideline for the Diagnosis and Treatment ofUlcerative Colitis with Integrated Chinese and Western Medicine. 2023. doi:10.1016/j.ims.2023.174524
13. Wang YF, Zhang JQ, Xu L, et al. Modified gegen qinlian decoction regulates Treg/Th17 balance to ameliorate dss-induced acute experimental colitis in mice by altering the gut microbiota. *Front Pharmacol*. 2021;12:22. doi:10.3389/fphar.2021.756978
14. Yang CK, Cheng JW, Zhu QW, et al. Review of the protective mechanism of paeonol on cardiovascular disease. *Drug Des Dev Ther*. 2023;17:2193–2208. doi:10.2147/dddt.S414752
15. Liu BH, Piao XH, Niu W, et al. Kuijieyuan decoction improved intestinal barrier injury of ulcerative colitis by affecting TLR4-dependent PI3K/AKT/NF-κB oxidative and inflammatory signaling and gut microbiota. *Front Pharmacol*. 2020;11:18. doi:10.3389/fphar.2020.01036
16. Dong YL, Fan H, Zhang Z, et al. Berberine ameliorates DSS-induced intestinal mucosal barrier dysfunction through microbiota-dependence and Wnt/β-catenin pathway. *Int J Biol Sci*. 2022;18(4):1381–1397. doi:10.7150/ijbs.65476
17. Zhang LL, Wei W. Anti-inflammatory and immunoregulatory effects of paeoniflorin and total glucosides of paeony. *Pharmacol Ther*. 2020;207:12. doi:10.1016/j.pharmthera.2019.107452
18. Liang S, Deng X, Lei L, et al. The comparative study of the therapeutic effects and mechanism of baicalin, baicalein, and their combination on ulcerative colitis rat. *Front Pharmacol*. 2019;10:15. doi:10.3389/fphar.2019.01466
19. Penglu W. Historical evolution and clinical application of huanglian ejiaotang. *Chin J Exp Traditional Med Formulae*. 2023. doi:10.13422/j.cnki.syfjx.20221311
20. Salort G, Alvaro-Bartolomé M, García-Sevilla JA. Pentobarbital and other anesthetic agents induce opposite regulations of MAP kinases p-MEK and p-ERK, and upregulate p-FADD/FADD neuroplastic index in brain during hypnotic states in mice. *Neurochem Int*. 2019;122:59–72. doi:10.1016/j.neuint.2018.11.008
21. Hou X, Zhu FF, Zheng WW, et al. Protective effect of *Schistosoma japonicum* eggs on TNBS-induced colitis is associated with regulating Treg/Th17 balance and reprogramming glycolipid metabolism in mice. *Front Cell Infect Microbiol*. 2022;12:13. doi:10.3389/fcimb.2022.1028899
22. Yan BF, Chen X, Chen YF, et al. Aqueous extract of paeoniae radix alba *(Paeonia lactiflora* Pall.) ameliorates DSS-induced colitis in mice by tunning the intestinal physical barrier, immune responses, and microbiota. *J Ethnopharmacol*. 2022;294:12. doi:10.1016/j.jep.2022.115365
23. Yan YX, Shao MJ, Qi Q, et al. Artemisinin analogue SM934 ameliorates DSS-induced mouse ulcerative colitis via suppressing neutrophils and macrophages. *Acta Pharmacol Sin*. 2018;39(10):1633–1644. doi:10.1038/aps.2017.185
24. Dong WR, Li YY, Liu TT, et al. Ethyl acetate extract of Terminalia chebula alleviates DSS-induced ulcerative colitis in C57BL/6 mice. *Front Pharmacol*. 2023;14:1229772. doi:10.3389/fphar.2023.1229772
25. Lefrancois L, Lycke N. Isolation of mouse small intestinal intraepithelial lymphocytes, Peyer's patch, and lamina propria cells. *Curr Protocol Immunol*. 2001;17:3–19.. doi:10.1002/0471142735.im0319s17
26. Hu Y, Tang J, Xie Y, et al. Gegen Qinlian decoction ameliorates TNBS-induced ulcerative colitis by regulating Th2/Th1 and Tregs/Th17 cells balance, inhibiting NLRP3 inflammasome activation and reshaping gut microbiota. *J Ethnopharmacol*. 2024;328:117956. doi:10.1016/j.jep.2024.117956
27. Goc J, Lv M, Bessman NJ, et al. Dysregulation of ILC3s unleashes progression and immunotherapy resistance in colon cancer. *Cell*. 2021;184(19):5015–+. doi:10.1016/j.cell.2021.07.029
28. Gu P, Zhu L, Liu Y, et al. Protective effects of paeoniflorin on TNBS-induced ulcerative colitis through inhibiting NF-kappaB pathway and apoptosis in mice. *Int Immunopharmacol*. 2017;50:152–160. doi:10.1016/j.intimp.2017.06.022
29. Renner P, Crone M, Kornas M, et al. Intracellular flow cytometry staining of antibody-secreting cells using phycoerythrin-conjugated antibodies: pitfalls and solutions. *Antibody Ther*. 2022;5(3):151–163. doi:10.1093/abt/tbac013
30. Jiao BB, Tang Y, Liu S, et al. Tetrandrine attenuates hyperoxia-induced lung injury in newborn rats via NF-κB p65 and ERK1/2 pathway inhibition. *Ann Transl Med*. 2020;8(16):13. doi:10.21037/atm-20-5573
31. Wang RK, Yang TY, Feng Q, et al. Integration of network pharmacology and proteomics to elucidate the mechanism and targets of traditional Chinese medicine Biyuan Tongqiao granule against allergic rhinitis in an ovalbumin-induced mice model. *J Ethnopharmacol*. 2024;318:14. doi:10.1016/j.jep.2023.116816
32. Gomez-Bris R, Saez A, Herrero-Fernandez B, et al. CD4 T-cell subsets and the pathophysiology of inflammatory bowel disease. *Int J Mol Sci*. 2023;24(3):26. doi:10.3390/ijms24032696
33. Liu YL, Zhou MY, Yang M, et al. *Pulsatilla chinensis* saponins ameliorate inflammation and DSS-induced ulcerative colitis in rats by regulating the composition and diversity of intestinal flora. *Front Cell Infect Microbiol*. 2021;11:11. doi:10.3389/fcimb.2021.728929
34. Luo YT, Wu J, Zhu FY, et al. Gancao xiexin decoction ameliorates ulcerative colitis in mice via modulating gut microbiota and metabolites. *Drug Des Dev Ther*. 2022;16:1383–1405. doi:10.2147/dddt.S352467
35. Wang X, Quan J, Xiu C, et al. Gegen Qinlian decoction (GQD) inhibits ulcerative colitis by modulating ferroptosis-dependent pathway in mice and organoids. *Chin Med*. 2023;18(1):110. doi:10.1186/s13020-023-00819-4
36. Hu J, Tong Y, Shen Z, et al. Gegen Qinlian decoction ameliorates murine colitis by inhibiting the expansion of Enterobacteriaceae through activating PPAR-γ signaling. *Biomed Pharmacother*. 2022;154:113571. doi:10.1016/j.biopha.2022.113571
37. Ma J, Zhang J, Wang Y, et al. Modified Gegen Qinlian decoction ameliorates DSS-induced chronic colitis in mice by restoring the intestinal mucus barrier and inhibiting the activation of γδT17 cells. *Phytomedicine*. 2023;111:154660. doi:10.1016/j.phymed.2023.154660
38. Ji LA, Wang SL, Wu S, et al. Paeoniflorin inhibits LPS-induced activation of splenic CD4+ T lymphocytes and relieves pathological symptoms in MRL/lpr mice by suppressing IRAK1 signaling. *Evid-Based Complement Altern Med*. 2022;2022:17. doi:10.1155/2022/5161890

39. Cai -W-W, Gao Y, Cheng J-W, et al. Berberine modulates the immunometabolism and differentiation of CD4+ T cells alleviating experimental arthritis by suppression of M1-exo-miR155. *Phytomedicine*. 2024;124:155255. doi:10.1016/j.phymed.2023.155255
40. Chen SK, Lin ZB, He TZ, et al. Topical application of tetrandrine nanoemulsion promotes the expansion of CD4+Foxp3+ regulatory T cells and alleviates imiquimod-induced psoriasis in mice. *Front Immunol*. 2022;13:12. doi:10.3389/fimmu.2022.800283
41. Fu YJ, Xu B, Huang SW, et al. Baicalin prevents LPS-induced activation of TLR4/NF-κB p65 pathway and inflammation in mice via inhibiting the expression of CD14. *Acta Pharmacol Sin*. 2021;42(1):88–96. doi:10.1038/s41401-020-0411-9
42. Liu C, Li YY, Chen YP, et al. Baicalein restores the balance of Th17/Treg cells via aryl hydrocarbon receptor to attenuate colitis. *Mediators Inflammation*. 2020;2020:19. doi:10.1155/2020/5918587
43. Rong WH, Wan NY, Zheng X, et al. Chrysin inhibits hepatocellular carcinoma progression through suppressing programmed death ligand 1 expression. *Phytomedicine*. 2022;95:10. doi:10.1016/j.phymed.2021.153867
44. Narula M, Lakshmanan U, Borna S, et al. Epigenetic and immunological indicators of IPEX disease in subjects with *FOXP3* gene mutation. *J Allergy Clin Immunol*. 2023;151(1):233–+. doi:10.1016/j.jaci.2022.09.013
45. Liu TJ, Shi YY, Du J, et al. Vitamin D treatment attenuates 2,4,6-trinitrobenzene sulphonic acid (TNBS)-induced colitis but not oxazolone-induced colitis. *Sci Rep*. 2016;6:10. doi:10.1038/srep32889
46. Ogino H, Fukaura K, Iboshi Y, et al. Role of the IL-23-T-bet/GATA3 Axis for the pathogenesis of ulcerative colitis. *Inflammation*. 2021;44(2):592–603. doi:10.1007/s10753-020-01358-y
47. Zhou LL, Lin XL, Ma XM, et al. Acetylcholine regulates the development of experimental autoimmune encephalomyelitis via the CD4+cells proliferation and differentiation. *Int J Neurosci*. 2020;130(8):788–803. doi:10.1080/00207454.2019.1706504
48. Spieler V, Ludwig MG, Dawson J, et al. Targeting interleukin-4 to the arthritic joint. *J Control Release*. 2020;326:172–180. doi:10.1016/j.jconrel.2020.07.005
49. Haneishi Y, Furuya Y, Hasegawa M, et al. Inflammatory bowel diseases and gut microbiota. *Int J Mol Sci*. 2023;24(4):13. doi:10.3390/ijms24043817
50. Quaglio AEV, Grillo TG, De Oliveira ECS, et al. Gut microbiota, inflammatory bowel disease and colorectal cancer. *World J Gastroenterol*. 2022;28(30):4053–4060. doi:10.3748/wjg.v28.i30.4053
51. Zhu SY, Han MZ, Liu SM, et al. Composition and diverse differences of intestinal microbiota in ulcerative colitis patients. *Front Cell Infect Microbiol*. 2022;12:13. doi:10.3389/fcimb.2022.953962
52. Zhao H, Ding TH, Chen YL, et al. Arecoline aggravates acute ulcerative colitis in mice by affecting intestinal microbiota and serum metabolites. *Front Immunol*. 2023;14:12. doi:10.3389/fimmu.2023.1197922
53. Li ZY, Lin LH, Liang HJ, et al. Lycium barbarum polysaccharide alleviates DSS-induced chronic ulcerative colitis by restoring intestinal barrier function and modulating gut microbiota. *Ann Med*. 2023;55(2):2290213. doi:10.1080/07853890.2023.2290213
54. Li M, Guo W, Dong Y, et al. Beneficial effects of celastrol on immune balance by modulating gut microbiota in experimental ulcerative colitis mice. *Genomics Proteomics Bioinf*. 2022;20(2):288–303. doi:10.1016/j.gpb.2022.05.002
55. Song X, Wang W, Liu L, et al. Poria cocos attenuated dss-induced ulcerative colitis via NF-κB signaling pathway and regulating gut microbiota. *Molecules*. 2024;29(9):2154. doi:10.3390/molecules29092154
56. Tarris G, de Rougemont A, Charkaoui M, et al. Enteric viruses and inflammatory bowel disease. *Viruses-Basel*. 2021;13(1):13. doi:10.3390/v13010104
57. Li LN, Liu Y, Zhang HC, et al. *Helicobacter pylori* infection reduces TAMs infiltration in a mouse model of AOM/DSS induced colitis-associated cancer. *PLoS One*. 2020;15(11):10. doi:10.1371/journal.pone.0241840